Effects of High-Order Nonlinearities on Freak Wave Generation in Random Sea States

Y. Q. Zhang and J. P. Hu†

Guangzhou Maritime University, Guangzhou, Guangdong, 510725, China
College of Harbour and Coastal Engineering, Jimei University. Xiamen, Fujian, 361021, China

†*Corresponding Author Email: hujp@scsio.ac.cn*

ABSTRACT

High-order nonlinearities may be an important cause of freak wave generation; however, it is still unclear how to stimulate the generation of freak waves in deep-water random waves. This study employs the modified fourth-order nonlinear Schrödinger equation (mNLSE) to simulate the occurrence of freak waves and analyses the influence of high-order nonlinearities on the evolution of random wave trains described initially by the JONSWAP spectrum. In the evolution of freak wave generation, variations in the linear and nonlinear terms of the mNLSE are displayed with the nonlinear growth of surface elevations. For comparison, the corresponding results from the cubic nonlinear Schrödinger equation (CSE) and the linear Schrödinger equation (LSE) are also obtained. Power spectra and spectral peakedness curves in the evolution of the wave train are also given to analyze the potential mechanism of freak wave formation. Additionally, the probabilities of freak wave appearances are estimated for different initial parameters and different governing equations. The results show that the fourth-order nonlinearity plays an important role in the generation of freak waves, but this single factor is not enough to generate freak waves, and freak wave occurrence is the contribution of multiple factors to the unstable evolution of the wave train. The higher-order nonlinearity, concentrated initial random phases, larger wave steepness, narrower initial spectral width, and smaller sideband instability parameter can increase the probability of freak wave generation.

Keywords: Freak waves; High-order nonlinearity; mNLSE; CSE; LSE; Random waves.

NOMENCLATURE

a	carrier amplitude	k_0	carrier wavenumber
A	dimensionless complex wave envelope of the first-order Stokes wave	m_0	0-order moment of spectrum
		M	frequency interval number
A'	complex wave envelope of the first-order Stokes wave	t	time coordinate
		T_p	spectral peak period
f	frequency	x	horizontal coordinate
f_0	spectral peak frequency	z	dimensionless vertical coordinate
f_H	high frequency limit	z'	vertical coordinate
f_j	the jth frequency	α	energy scale parameter
f_L	low frequency limit	γ	peak enhancement factor
g	gravity acceleration	ε	wave steepness
h	dimensionless water depth	ζ	dimensionless wave surface displacement
h'	water depth	ζ'	wave surface displacement
H_{cr}	wave crest height	η	dimensionless coordinates corresponding to x
H_d	zero downcrossing wave height	λ	scale factor
H_f	zero upcrossing wave height	ξ	dimensionless coordinates corresponding to t
H_{f+1}	neighboring backward wave height of H_f	σ	peak shape parameter
H_{f-1}	neighboring front wave height of H_f	ϕ	dimensionless potential of the induced mean current
H_s	significant wave height		
H_{max}	maximum zero upcrossing wave height	ϕ'	potential of the induced mean current
i	imaginary unit	ψ	phase function
j	integer	ω	carrier frequency corresponding to k
k	wavenumber		

1. INTRODUCTION

Freak waves are special extreme waves in the ocean. Their original accounts came from survivors of marine accidents. People began to be concerned about this kind of large wave in recent decades. Then, various incidents of ships and nearshore persons encountering freak waves were reported gradually (Liu and MacHutchon 2006; Chien *et al.* 2002; Lavrenov 1998; Tian 2006; Kharif and Pelinovsky 2003; Warwick 1996; Graham 2000; Didenkulova *et al.* 2006; Nikolkina and Didenkulova 2011). Recently, the most likely freak wave incident occurred on the beach of Zhangzhou, Xiamen, Fujian Province, China, on August 14th, 2021, in which an abrupt giant wave swept away 17 persons on the beach and caused 11 deaths (http://cnews.chinadaily.com.cn/a/202108/16/WS61 19c179a3101e7ce975ec20.html). All the accidents are so shocking that many researchers are paying much more attention to freak waves.

At present, the most classic freak wave is the "New Year Wave" that attacked the Draupner oil platform in the North Sea on January 1st, 1995 (Haver and Andersen 2000; Haver 2004; Walker *et al.* 2004). Its wave height H_f =25.6 m and H_d =25.0 m, its wave crest height H_{cr}=18.5 m and its period is approximately 12 s, while its neighboring heights are H_{f-1}=11.6 m and H_{f+1}=6.8 m and the significant wave height is H_s=11.9 m in the background wave train. Thus H_{cr}/H_f =0.72, H_f/H_s =2.15, H_f/H_{f-1}=2.21, H_f/H_{f+1}=3.76 and H_d/H_f =0.98. Some of them are much higher than the thresholds of the rigorous freak wave definition given by Klinting and Sand (1987), and these ratios are also obviously different from those of ordinary waves, showing obvious nonlinear properties.

Generally, wave nonlinearity has an important effect on the unstable evolution of wave trains, which affects not only the internal energy distribution among different components in random waves but also the symmetry of the wave shape. Veltcheva and Soares (2016) analyzed the nonlinearity of measured freak waves by the Hilbert–Huang transform method and proposed that a larger intrawave frequency modulation is associated with a higher asymmetry of the wave profile. Cui and Zhang (2011) and Hu and Zhang (2014) carried out wavelet transforms to analyze the energy evolution of wave trains and found that the nonlinearity effect leads to the shift of energy to high frequencies to form freak waves. Mori and Yasuda (2002) used a high-order nonlinear model and its second-order approximated model together with the Wallops spectrum to study the effect of spectrum width and water depth on the stability of random waves and believed that higher-order nonlinearities beyond the third order stimulate the chaotic evolution of Fourier spectral energy in deep-water waves, which can produce a single and extreme large wave with a remarkable peak height, and higher-order nonlinearities can be regarded as a reason for freak waves in deep water. Thus, the influence of high-order nonlinearities on the prediction of maximum wave height and freak waves should be considered independently of spectral width.

Many parameters in the initial wave trains also affect the formation of freak waves in their nonlinear evolution. Kashima and Mori (2019) pointed out that the third-order nonlinearity at greater water depths remarkably affects the random wave height distribution on the slope. Onorato *et al.* (2001) used the CSE to study the occurrence of freak waves in random oceanic sea states characterized by the JONSWAP spectrum, revealing that large values of the Phillips parameter and enhancement coefficient increase their occurrence probability. Shemer *et al.* (2010a) investigated the spatial evolution of unidirectional random waves in a 300 m long wave tank and with the CSE and the mNLSE as the theoretical models and indicated that the statistical characteristics of the random wave field depend on the local width of the frequency spectrum and deviate from Gaussian statistics: the probability of extremely large (the so-called freak) waves is highest when the local spectral width attains a maximum. Shemer *et al.* (2010b) used the Gaussian spectrum, JONSWAP spectrum and rectangular spectrum to study the influence of spectrum width on the statistical parameters of nonlinear random waves in this large wave channel and pointed out that when the initial spectrum was narrow enough, freak waves would appear relatively frequently and the probability of freak waves for a wide initial spectrum is lower than that given by the Rayleigh distribution. Xia *et al.* (2015) performed a numerical simulation of freak wave generation in random sea states given by the JONSWAP spectrum with the mNLSE model and an instability indicator of the Benjamin-Feir index and proposed that a narrow spectrum and small significant wave height are helpful to form freak waves. Kirezci *et al.* (2021) employed the fully nonlinear Chalikov-Sheinin (CS) model and the high-order spectral model to study the probability of freak waves caused by modulation instability, which is indicated by three parameters, under the wave conditions described by the JONSWAP spectrum. The occurrence probabilities of freak waves are shown in the contour line charts against the Phillips parameter-enhancement coefficient plane. When the Phillips parameter is within the range of (0.001, 0.020), the probability generally changes in a single peak, which first increases and then decreases. When the enhancement coefficient is in the range of (1, 7), the probability tends to increase. It is concluded that steepness and bandwidth are two controlling parameters in freak wave formation and that their combination can further instigate or limit modulation instability. Janssen (2003) used the Zakharov equation to investigate nonlinear four-wave interactions and freak waves and proposed that a narrower spectrum and larger wave steepness are favorable for the appearance of freak waves, while it is sensitive to initial random phases. Gramstad and Bitner-Gregersen (2019) also proposed that steepness is a key parameter for the probability of extreme and freak waves after analyzing the relation between spectral parameters

(H_s, T_p, steepness, and bandwidth) and kurtosis. Zhang *et al.* (2016) discussed statistical properties of nonlinear wave series with the nonlinear CS model and the temporal version of MNLS and revealed that both numerical models are able to capture the critical features (e.g., low probability) of mechanically generated long-crested waves induced by the nonlinear modulation except for the exceedance distribution of wave height and the more subtle features.

These studies show that NLS-type models are suitable for the investigation of freak waves. The nonlinearity of waves and the variation in component wave energy can influence the formation of freak waves, and many factors in the initial wave trains, such as wave steepness, spectral width, and spectral parameters, also affect the probability of freak waves. However, they partially emphasized the effects of some factors on freak wave generation.

On the basis of existing investigations, this paper studies the influence of higher-order nonlinearities together with other relevant factors on freak wave formation. The mNLSE model is selected to simulate the generation of freak waves in deep and random sea states. The corresponding results from the CSE model and the LSE model are also given to analyze the effect of multiple factors on the appearance of freak waves.

2. NUMERICAL MODELS

2.1 Governing Equations and Numerical Solutions

The dimensionless mNLSE (Lo and Mei 1985) in the moving coordinate system with group velocity is shown in Eqs. (1) and (2), which controls the evolution of the deep-water complex wave envelope characterized by the narrow spectrum.

$$\frac{\partial A}{\partial \eta} + i\lambda^2 \frac{\partial^2 A}{\partial \xi^2} + i|A|^2 A = -8\varepsilon\lambda |A|^2 \frac{\partial A}{\partial \xi} - 4i\varepsilon\lambda A \frac{\partial \phi}{\partial \xi}\bigg|_{z=0} \quad (1)$$

$$\begin{cases} 4\dfrac{\partial^2 \phi}{\partial \xi^2} + \dfrac{\partial^2 \phi}{\partial z^2} = 0, & -h < z < 0 \\[2mm] \dfrac{\partial \phi}{\partial z} = \dfrac{\partial |A|^2}{\partial \xi}, & z = 0 \\[2mm] \dfrac{\partial \phi}{\partial z} = 0, & z = -h \end{cases} \quad (2)$$

where $\varepsilon=ka$, the following transformations in Eq. (3) exist between the physical variables and dimensionless variables.

$$\begin{cases} A' = aA, \ \zeta' = a\zeta, \ \phi' = \omega a^2\phi, \ \varepsilon^2 kx = \eta \\ \varepsilon\omega\lambda (2kx/\omega - t) = \xi, \ \varepsilon\lambda kz' = z, \ \varepsilon\lambda kh' = h \end{cases} \quad (3)$$

where λ is the scale factor that adjusts the calculation domain in ξ to 2π and x is the horizontal coordinate of the wave propagation direction. Thus, (ξ, η, z) is a new coordinate system transformed from the dimensional coordinate system (t, x, z').

Equation (1) is a higher-order nonlinear equation and can be solved quickly with Eq. (2) through a split-step pseudospectral method (Lo and Mei 1985). According to the evolution of the complex envelope in space, the wave surface displacement can be calculated as Eq. (4).

$$\zeta(\xi,\eta) = \varepsilon^2 \lambda \frac{\partial \phi}{\partial \xi}\bigg|_{z=0} + \frac{1}{2}\left\{\left(A - i\varepsilon\lambda \frac{\partial A}{\partial \xi} - \frac{3\varepsilon^2}{8}|A|^2 A\right)e^{i\psi}\right.$$
$$\left. + \left(\frac{\varepsilon}{2}A^2 - 2i\varepsilon^2\lambda A \frac{\partial A}{\partial \xi}\right)e^{2i\psi} + \left(\frac{3\varepsilon^2}{8}A^3\right)e^{3i\psi} + c.c.\right\} \quad (4)$$

where $\psi=-\eta/\varepsilon^2+\xi/\varepsilon\lambda$ is the phase function of the carrier wave and c.c. represents a complex conjugate.

The right part of Eq. (1) is the fourth-order nonlinear term, and the third term on the left is the third-order nonlinear term. Letting the fourth-order term be 0, the mNLSE becomes the CSE, and only letting the first two terms on the left side be 0, it becomes the LSE. In the computation, the free wave surface evolved through the LSE is $\{Ae^{i\psi}+c.c.\}/2$, and the wave surface simulated with the CSE is the truncated term of Eq. (4) to the second harmonic term.

2.2 Initial Wave Conditions

The typical sea states, described by the JONSWAP spectrum (Yu and Liu, 2011), are selected as initial random wave conditions. This spectrum is expressed as follows:

$$S(f) = \frac{\alpha g^2}{(2\pi)^4} \frac{1}{f^5} \exp\left[-1.25\left(\frac{f_0}{f}\right)^4\right]\gamma^{\exp\left[-(f-f_0)^2/2\sigma^2 f_0^2\right]} \quad (5)$$

where α is also known as the Phillips parameter. If $f \leq f_0$, $\sigma = 0.07$, and if $f > f_0$, $\sigma=0.09$.

In the simulation, f_0 is set as the carrier frequency, k_0 is the corresponding wavenumber, the wave steepness $\varepsilon=(k_0 H_s)/2$ and the significant wave height $H_s = 4.0\sqrt{m_0}$. Based on the linear superposition law, the initial wave surface is assumed to be composed of M monochromatic waves, and its dimensionless form is as follows:

$$\zeta(\xi,0) = \frac{2}{H_s}\sum_{j=1}^{M} C_j \cos\left(\frac{\tilde{f}_j}{f_0}\frac{\xi}{\lambda\varepsilon} + \varphi_j\right) \quad (6)$$

where φ_j is a random number distributed in (0, 2π). Most of the JONSWAP spectral energy is distributed in the frequency range (f_L, f_H), and the rest is omitted. This frequency range is divided into M intervals, where its interval $\Delta f_j = f_{j+1} - f_j$ and $\tilde{f}_j = (f_{j+1} + f_j)/2$ are set, and then $C_j = \sqrt{2S(\tilde{f}_j)\Delta f_j}$, where $j = 1,2,\cdots,M$, $M = 50$, $f_1=f_L$ and $f_{51}=f_H$.

The corresponding dimensionless initial complex wave envelope is constructed as follows:

$$A(\xi,0) = \frac{2}{H_s}\sum_{j=1}^{M} C_j \exp\left\{i\left[\frac{(\tilde{f}_j - f_0)}{f_0}\frac{\xi}{\lambda\varepsilon} + \varphi_j\right]\right\} \quad (7)$$

Table 1 Parameters of the initial wave trains

Parameters	α	γ	f_0, Hz	f, Hz	λ	M
Value	0.0081, 0.0162	4, 7	0.1	$0.5\,f_0 \sim 1.6\,f_0$	0.1~1.2	50

where all relevant parameters except random phases are selected as shown in Table 1. The random phases are from the products of random numbers in the range of (0, 1) and 2π, which are displayed in Fig. 1.

(a)   Group 1

(b) Group 2

(c) Group 3
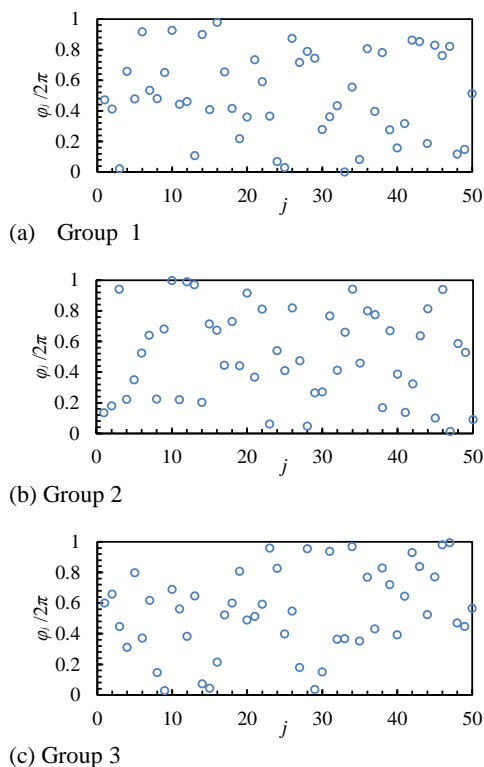
Fig. 1. Three groups of random numbers for the initial phase.

3. NUMERICAL RESULTS AND ANALYSIS
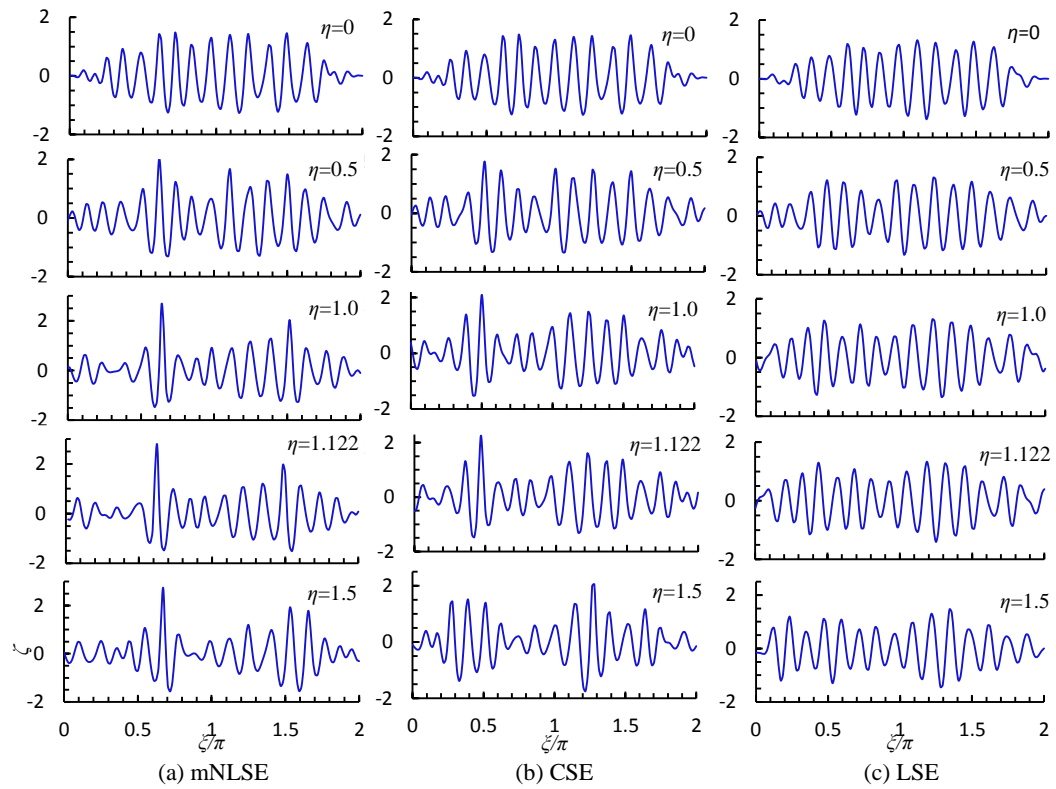
3.1 Generation of Freak Waves

Mei (1992) pointed out that sideband instability, namely, Benjamin-Feir instability, exists in the evolution of the slow modulated periodic wave train, which can cause its amplitude to increase exponentially in the local domain.

It is known that sideband instability develops rapidly when the wave steepness is large (Lo and Mei 1985). Therefore, JONSWAP spectral parameters α=0.0162 and γ=7 were set to simulate the initial wave train, and this spectrum is so high and steep that its wave steepness is large. The initial random phases come from the random numbers of Group 1 in Fig. 1, which are mainly used in our simulations except for special instructions. The simulated results for λ=0.4 are selected to display the effect of high-order nonlinearity on freak wave

generation. In the evolution of the wave train, the zero upper-crossing method is employed to estimate the wave height, and the definition given by Klinting and Sand (1987) is used to determine the occurrence of freak waves.

Figure 2 (a) shows the evolution of the initial wave train by the mNLSE. The initial wave surface processed periodically consists of a series of wave groups. In the evolution, the second wave group on the left becomes increasingly higher, and their adjacent wave displacements gradually decrease. The group at η=1.122 grows into a freak wave group with a sharp and thin crest and bilateral asymmetry troughs. There are corresponding extreme waves in the wave trains before and after the generation of freak waves. Although they are not determined as freak waves because they cannot simultaneously meet the three conditions of freak waves, they are still dangerous waves.Figures 2 (b) and (c) show the corresponding wave trains from evolutions of the same initial complex envelope through the LSE and CSE, respectively. In Fig. 2 (b), the energy of the wave train in the evolution gradually shifts to the second wave group on the left so that it continuously increases, but its growth speed is less than that obtained through the mNLSE. At η=1.122, it evolves into an extreme asymmetric wave group; however, the extreme wave does not reach the threshold of a freak wave. In Fig. 2 (c), the evolution of the wave surface through the LSE is similar to the results of the CSE, but there is no distinguished wave surface growth, and no extreme wave appears.

Figure 3 shows the variations in the modulus of each term in the first formula for the mNLSE, CSE and LSE corresponding to Fig. 1. In Eq. (1), the first and second terms of the mNLSE are linear terms, the third term is a third-order nonlinear term, and the fourth and fifth terms are fourth-order nonlinear terms. As shown in Fig. 3(a), at η=0, the amplitude of the fourth term is larger and that of the fifth term is smaller in the second wave group on the left. With the increase in this wave group height, the amplitude of the fourth term varies rapidly in the form of a single peak, always has a maximum value at the time of the large wave, and reaches the extreme value in the whole evolution at the time of freak wave generation. The amplitude variations of other terms are similar to that of the fourth term, but their levels gradually decrease from the second term, third term, and first term to the fifth term at the time of large wave generation. In Fig. 3(b), the amplitude of the third-order nonlinear term does not have an obvious change in the initial wave train, but it has a remarkable single-peak growth at the moment of the asymmetric big wave in the evolution, while the second linear term also has a significant peak growth, so it is determined that the third-order nonlinearity plays an important role in the asymmetric growth of the large wave. Fig. 3(c)

(a) mNLSE (b) CSE (c) LSE

Fig. 2. Wave train evolution for freak wave generation through the mNLSE and corresponding evolutions through the CSE and LSE.

(a) mNLSE (b) CSE (c) LSE
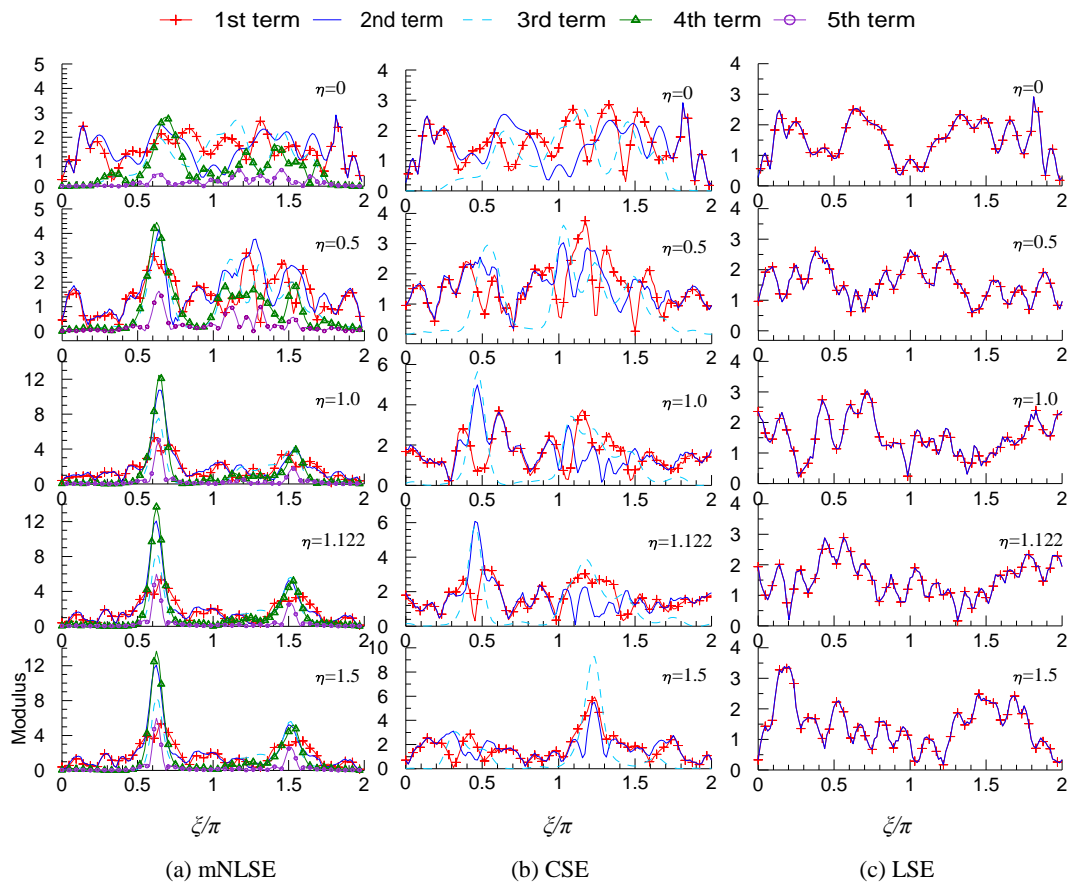
Fig. 3. Variations in each term modulus in the three Schrödinger equations corresponding to Fig. 2.

exhibits the amplitude evolutions of linear terms in the LSE. In the whole evolution, their amplitudes have not changed significantly.

Evolutions of each order term of the three Schrödinger equations and variations in the corresponding wave elevations indicate that the fourth-order nonlinearity from the fourth term of the mNLSE and the third-order nonlinearity lead to the rapid and asymmetric increase in the large wave height, while the second linear term also effectively promotes the generation of large waves, so the occurrence of freak waves mainly arises from the contribution of the fourth-order and third-order nonlinearities and linearity, and the fourth-order nonlinearity plays a more important role than the third-order nonlinearity.

3.2 Spectrum Evolution

In the evolution of the wave train, the frequency spectrum is calculated by means of the fast Fourier transform method, and its spectrum width is estimated by using the peakedness Q_p. A larger Q_p denotes a narrower spectrum width.

$$Q_p = \frac{2}{m_0^2} \int_0^{f_H} f s^2(f) df \qquad (8)$$

Figure 4(a) shows variations in the frequency spectrum for the wave train evolution through the mNLSE. When the wave train propagates from $\eta = 0$ to $\eta = 1.122$, the energy of the spectral peak continuously decreases and mainly shifts to the high frequency components far away from the peak frequency, especially for the position of the freak wave. At $\eta = 1.5$, the peak values decrease considerably and mainly shift to the frequency band near the spectral peak, corresponding to an asymmetric large wave in Fig. 1. For the wave train evolution via the CSE, the energy of the spectrum peak has a smaller decline and a slight shift to the high frequency components, as shown in Fig. 4(b). When the initial wave train evolves through the LSE, its frequency spectrum remains basically unalterable in the whole evolution, as shown in Fig. 4(c).

Figure 5 exhibits the peakedness curves of the above spectra. In the evolution of the initial wave train through the LSE, the peakedness curves in Fig. 5(c) change very slightly, so the spectral width can be considered to be unchanged. For the wave train evolution controlled by the CSE, the peakedness curves in Fig. 5(b) drop gradually with the appearance of high waves with asymmetric crests and troughs, and thus, the spectral width increases correspondingly. The peakedness curves in Fig. 5(a) computed via wave trains from the mNLSE have a similar decline to that of the CSE, but their declining range is larger.

For the mNLSE model, variations in the spectra and peakedness curves show that the fourth-order nonlinearity strengthens the shift of the spectrum peak energy to the high-frequency components, which causes the generation of asymmetric extreme waves, such as freak waves. The CSE model gives similar but weakened outcomes.

Although the wavelet spectrum method is more suitable for analyzing freak wave trains in the time and frequency domains (Chien *et al.* 2002), here, the energy spectrum method can still give similar results for the generation of freak waves to those from Cui and Zhang (2011) and Hu and Zhang (2014).
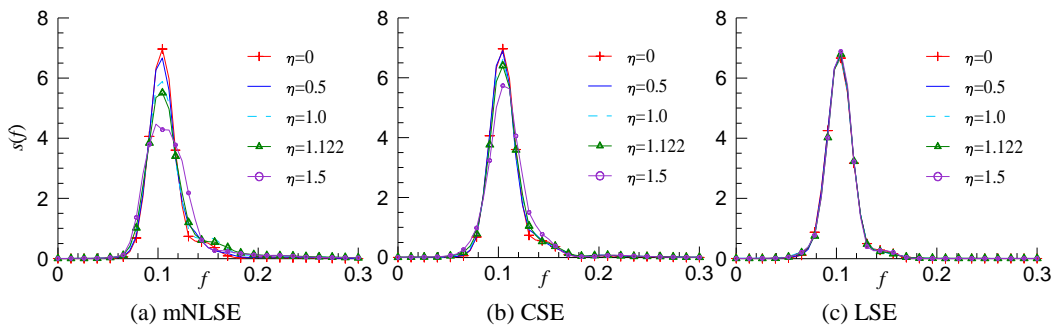

Fig. 4. Variation in the power spectrum for each wave train corresponding to Fig. 2.
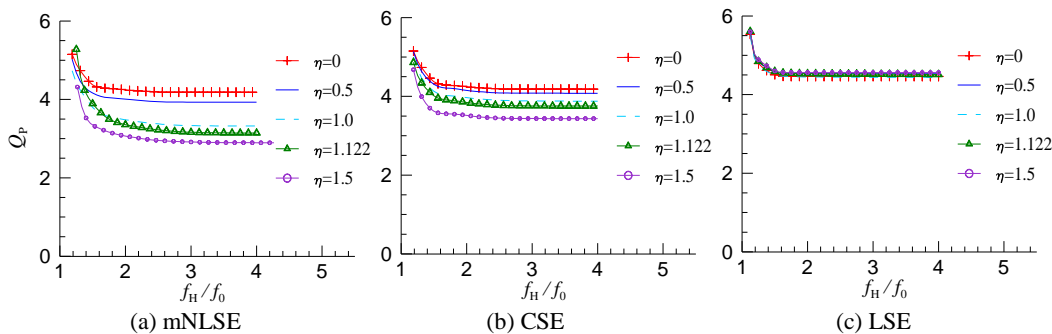

Fig. 5. Variation in spectral peakedness corresponding to Fig. 4.

3.3 Freak Wave Generation Probabilities

In these computations, the generation of freak waves is sensitive to initial random phases, so three groups of random numbers in Fig. 1, α=0.0162, γ=7 and the mNLSE are selected to study the effect of initial random phases on the freak wave formation. Fig. 6 displays the probabilities of different cases. The probability of freak wave occurrences in the evolution decreases with the growth of λ, and no freak wave occurs when λ>0.9. For the initial random phases of Group 1, the probability of freak wave occurrences is the largest. The probability for Group 2 is in the middle. For Group 3, freak waves appear only when λ=3. Therefore, the following simulations are carried out with the initial random phases of Group 1.

To analyze the effect of initial random phases on freak wave formation, random numbers are divided into 10 intervals with an interval of 0.1. The percentage of the number in every interval to the total number is shown in Fig. 7 for each random phase group. For Group 1, 18% of the random numbers are between 0.4 and 0.5. For Group 2, 16% of the random numbers are between 0.3 and 0.4, and 18% of the random numbers are between 0.5 and 0.6. Therefore, the relative concentration of random initial phases may be the reason for the higher probability of freak wave generation.
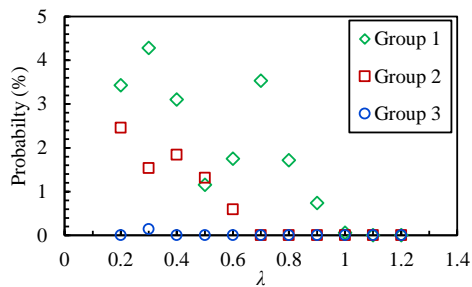

Fig. 6. Freak wave occurrence probability for three groups of initial random phases.
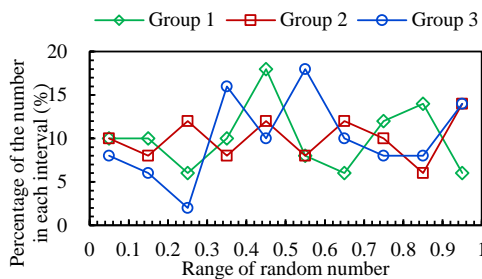

Fig. 7. Percentage of the number of random numbers in each interval.

To further determine the effect of nonlinearity on the occurrence of freak waves, evolutions of the same initial wave train are performed to estimate the probability of freak waves in space with the three Schrödinger equations employed. The results are shown in Fig. 8, except for the probabilities of cases for α=0.0081 and γ=4, which are all equal to 0.

(a) α=0.0162, γ=7

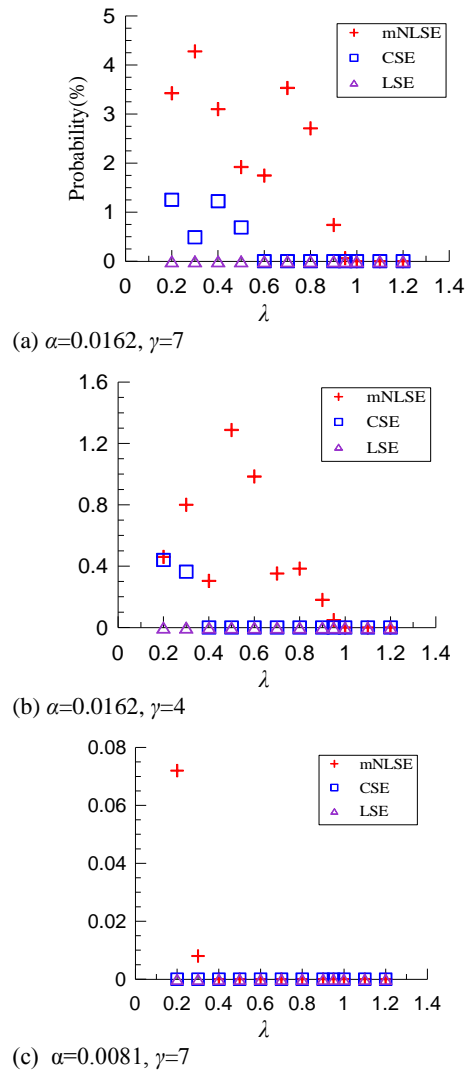(b) α=0.0162, γ=4

(c) α=0.0081, γ=7

Fig. 8. Comparisons of the freak wave occurrence probability with the mNLSE, CSE and LSE employed for different spectral parameters.

Figure 8 (a) shows the cases for spectral parameters α=0.0162 and γ=7. When the mNLSE is applied, the probabilities of freak wave occurrence are the largest among the simulations through the three equations. The maximum probability is 4.28%, and freak waves occur in the scale factor range of $0.2 \leq \lambda \leq 0.95$. When the CSE is employed, the corresponding occurrence probabilities decrease more than when the mNLSE is employed, the maximum probability is 1.25%, and the scale factor range of freak wave occurrence is $0.2 \leq \lambda \leq 0.5$. When the LSE is used, no freak wave appears in the evolution of wave trains. In Fig. 8 (b), the spectral parameters are set to α=0.0162 and γ=4. When the mNLSE is selected as the governing equation, the probabilities and the range of the scale factor for freak wave generation are similar to the cases of γ=7 for different λ values, but the probabilities drop considerably, and the maximum value is 1.29%. When the CSE is employed, the occurrence probability still decreases with increasing scale

factor λ, whose range of freak wave occurrence is $0.2 \leq \lambda \leq 0.3$, where the maximum occurrence probability is 0.44%. For the LSE model, freak waves do not appear in the evolution of the wave train. In Fig. 8 (c), where $\alpha=0.0081$, $\gamma=7$, and the mNLSE is selected as the governing equation, the probabilities for freak wave generation are very low, with a maximum value of 0.07%, and freak waves occur in the scale factor range of $0.2 \leq \lambda \leq 0.3$. When the CSE and LSE are employed, there is no freak wave in the simulations. Therefore, the fourth-order nonlinearity can increase the freak wave occurrence probability more than the third-order nonlinearity.

For the same α, the JONSWAP spectrum becomes narrow, and the wave steepness grows with increasing γ. For the same γ, according to the spectrum peakedness formula in (8), the spectrum width does not vary with α, but the wave steepness grows with increasing α, as shown in Table 2. Comparing Fig. 8 (a) with (b) and comparing Fig. 8 (c) with the probabilities of cases of $\alpha=0.0081$ and $\gamma=4$, the probability of freak wave occurrence increases with increasing γ or decreasing spectrum width. Comparing Fig. 8 (a) with (c) and comparing Fig. 8 (b) with the results of cases of $\alpha=0.0081$ and $\gamma=4$, the probability of freak waves increases with increasing α or wave steepness. These results are consistent with some numerical and experimental findings given by Onorato *et al.* (2001) and Shemer *et al.* (2010b).

It is known that sideband instability is related to wave steepness and wave steepness ε is related to spectral parameters α and γ. For the mNLSE model, according to the sideband instability criterion given by Lo and Mei (1985), the sideband instability ranges are different for different values of α and γ, as shown in Table 2, which can become large with the decrease in ε. For the CSE model, according to the sideband instability condition given by Onorato *et al.* (2001), sideband instability affects the evolution of the wave train in the range of $0 < \lambda < \sqrt{2}$. In all the evolutions of wave trains, there is no freak wave when the scale factor is larger than 1.0, as shown in Fig. 8. When the scale factor exceeds the sideband instability range or in the cases of $\alpha=0.0081$ and $\gamma=7$, no freak wave appears in any of the simulations. There is no freak wave occurring in the linear evolution of the wave train. Therefore, sideband instability plays an important role in the generation of freak waves, and the probability of freak wave occurrence decreases with increasing scale factor overall.

4. CONCLUSIONS

The occurrences of freak waves are numerically carried out through the mNLSE in random sea states characterized by the JONSWAP spectrum. For comparison, the same simulations are also performed with the CSE and LSE. Variations in the wave trains and nonlinear and linear terms of the three equations are analyzed and compared to determine the effect of higher-order nonlinearity on freak wave generation. The curves and widths of the

Table 2 Wave steepness and sideband instability ranges for different spectrum parameters

α	γ	ε	mNLSE	CSE
0.0162	7	0.163	$0 < \lambda < 1.125$	
0.0162	4	0.139	$0 < \lambda < 1.163$	$0 < \lambda < \sqrt{2}$
0.0081	7	0.115	$0 < \lambda < 1.202$	
0.0081	4	0.098	$0 < \lambda < 1.231$	

power spectra for the above evolutions of wave trains are estimated to reveal the energy transfer characteristics of the higher-nonlinearity effect on the freak wave appearance. The probabilities of freak wave occurrence in space are also computed for different parameters to analyze how they affect the formation of freak waves. Thus, the following conclusions can be drawn:

1) In the evolution of freak wave generation, fourth-order nonlinearity plays a key role in the nonlinear growth of the wave surface, and linearity and third-order nonlinearity also have an important effect.

2) The fourth-order nonlinearity causes a larger shift of the spectrum peak energy to the higher frequency components and a wider spectrum than the evolution results of the third-order nonlinearity. This energy transfer characteristic may be the internal cause of freak waves.

3) Initial phase modification is helpful for the generation of freak waves. The relative concentration of random initial phases can increase the probability of freak wave generation

4) The higher-order nonlinearity, larger wave steepness, narrower initial spectrum and smaller sideband instability parameter can increase the probability of freak wave formation.

5) It is very difficult to generate freak waves only by the linear evolution of waves.

On the whole, the fourth-order nonlinearity plays a very important role in the generation of freak waves, but a single factor is not enough to generate freak waves. The freak wave is the product of many factors that are beneficial to the generation of nonlinear large waves. It is difficult for realistic random wave trains to evolve into freak waves, and wave groupiness has an important influence on the generation of freak waves. Therefore, the wave group needs to be considered in further analyses.

ACKNOWLEDGMENTS

REFERENCES

Chien, H., C. C. Kao and L. Z. H. Chuang (2002). On the characteristics of observed coastal freak

waves. *Coastal Engineering Journal* 44(4), 301-319.

Cui, C. and N. Zhang (2011). Freak wave simulation based on nonlinear model and the research on the time-frequency energy spectrum of simulation results. *Marine Science Bulletin* 13 (1), 25-39.

Didenkulova, I. I., A. V. Slunyaev, E. N. Pelinovsky and C. Kharif (2006). Freak waves in 2005. *Natural Hazards and Earth System Sciences* 6(6), 1007–1015.

Graham, D. M. (2000). NOAA vessel swamped by rogue wave. *Oceanspace* 284.

Gramstad, O. and E. Bitner-Gregersen (2019). Predicting extreme waves from wave spectral properties using machine learning. *International Conference on Ocean, Offshore and Arctic Engineering*. Glasgow, Scotland, UK, 3, 1–10.

Haver, S. (2004). A Possible Freak Wave Event Measured at the Draupner Jacket January 1 1995. *Rogue waves 2004*, Brest, France, 1-8.

Haver, S. and J. O. Andersen (2000). Freak waves: rare realizations of a typical population or typical realizations of a rare population? *Proceedings of the tenth international offshore and polar engineering conference*, Seattle, USA, 3, 123-130.

Hu, J. and Y. Zhang (2014). Analysis of Energy Characteristics in the Process of Freak Wave Generation, *China Ocean Engineering* 28(2), 193 – 205.

Janssen P. A. E. M. (2003). Nonlinear Four-Wave Interactions and Freak Waves. *Journal of Physical Oceanography* 33(4), 863－884.

Kashima, H. and N. Mori (2019). Aftereffect of high-order nonlinearity on extreme wave occurrence from deep to intermediate water, *Coastal Engineering* 153, 1-14.

Kharif, C. and E. Pelinovsky (2003). Physical mechanisms of the rogue wave phenomenon. *European Journal of Mechanics B/Fluids* 22(6), 603-634.

Kirezci C., A. V. Babanin and D. V. Chalikov (2021). Modelling rogue waves in 1D wave trains with the JONSWAP spectrum, by means of the High Order Spectral Method and a fully nonlinear numerical model. *Ocean Engineering* 231(108715), 1-14.

Klinting, P. and S. Sand (1987). Analysis of prototype freak waves. *Coastal Hydrodynamics*, ASCE, 618-632.

Lavrenov, I. V. (1998). The wave energy concentration at the Agulhas current of South Africa, *Natural Hazards* 17, 117-127.

Liu, P. L. and K. R. MacHutchon (2006). Are there different kinds of rogue waves? *The 25th International Conference on Offshore Mechanics and Arctic Engineering,* Hamburg, Germany, 1-6.

Lo, E. and C. C. Mei (1985). A numerical study of water-wave modulation based on a higher-order nonlinear Schroedinger equation. *Journal of Fluid Mechanics* 150, 395- 416.

Mei, C. C. (1992). *The applied dynamics of ocean surface waves*. World Scientific Publishing Co. Pte. Ltd, Singapore.

Mori, N. and T. Yasuda (2002). Effects of high-order nonlinear interactions on unidirectional wave trains. *Ocean Engineering* 29(10), 1233–1245.

Nikolkina, I. and I. Didenkulova (2011). Rogue waves in 2006-2010. *Natural Hazards and Earth System Sciences* 11, 2913-2924.

Onorato, M., A. R Osborne., M. Serio and S. Bertone (2001). Freak waves in random oceanic sea states. *Physical review letters* 86(25), 5831-5834.

Shemer, L., A. Sergeeva and A. Slunyaev (2010a). Applicability of envelope model equations for simulation of narrow-spectrum unidirectional random wave field evolution: experimental validation. *Physics of Fluids* 22 (016601),1-9.

Shemer, L., A. Sergeeva and D. Liberzon (2010b). Effect of the initial spectrum on the spatial evolution of statistics of unidirectional nonlinear random waves. *Journal of Geophysical Research* 115 (C12039), 1-12.

Tian, G. (2006). Analysis and prevention of abnormal waves along the coast of South Africa. *Marine Technology* 1, 21-22. (In Chinese)

Veltcheva, A. and C. Guedes Soares (2016). Nonlinearity of abnormal waves by the Hilbert–Huang Transform method. *Ocean Engineering* 115, 30－38.

Walker, D. A. G., P. H. Taylor and R. E. Taylor (2004). The shape of large surface waves on the open sea and the Draupner New Year wave. *Applied Ocean Research* 26 (3-4), 73-83.

Warwick, R. W. (1996). Hurricane 'Luis', the Queen Elizabeth 2 and a Rogue Wave. *Marine Observer* 66, 134.

Xia, W., Y. Ma and G. Dong (2015). Numerical simulation of freak waves in random sea state. *Procedia Engineering* 116, 366 – 372.

Yu, Y. and S. Liu (2011). *Random Wave and Its Applications for Engineering*. Dalian University of Technology Press, Dalian, China. (In Chinese)

Zhang, H. D., C. Guedes Soares, D. Chalikov and A. Toffoli (2016). Modeling the spatial evolutions of nonlinear unidirectional surface gravity waves with fully nonlinear numerical method. *Ocean Engineering* 125, 60–69.